Title

Fusobacterium nucleatum subsp. nucleatum RadD binds Siglec-7 and inhibits NK cell-mediated cancer cell killing.

Journal

iScience, 27(6)

Authors

Galaski, Johanna
Rishiq, Ahmed
Liu, Mingdong
et al.

Publication Date

2024-06-21

DOI

10.1016/j.isci.2024.110157

iScience

CellPress
OPEN ACCESS

Article

Fusobacterium nucleatum subsp. *nucleatum* RadD binds Siglec-7 and inhibits NK cell-mediated cancer cell killing

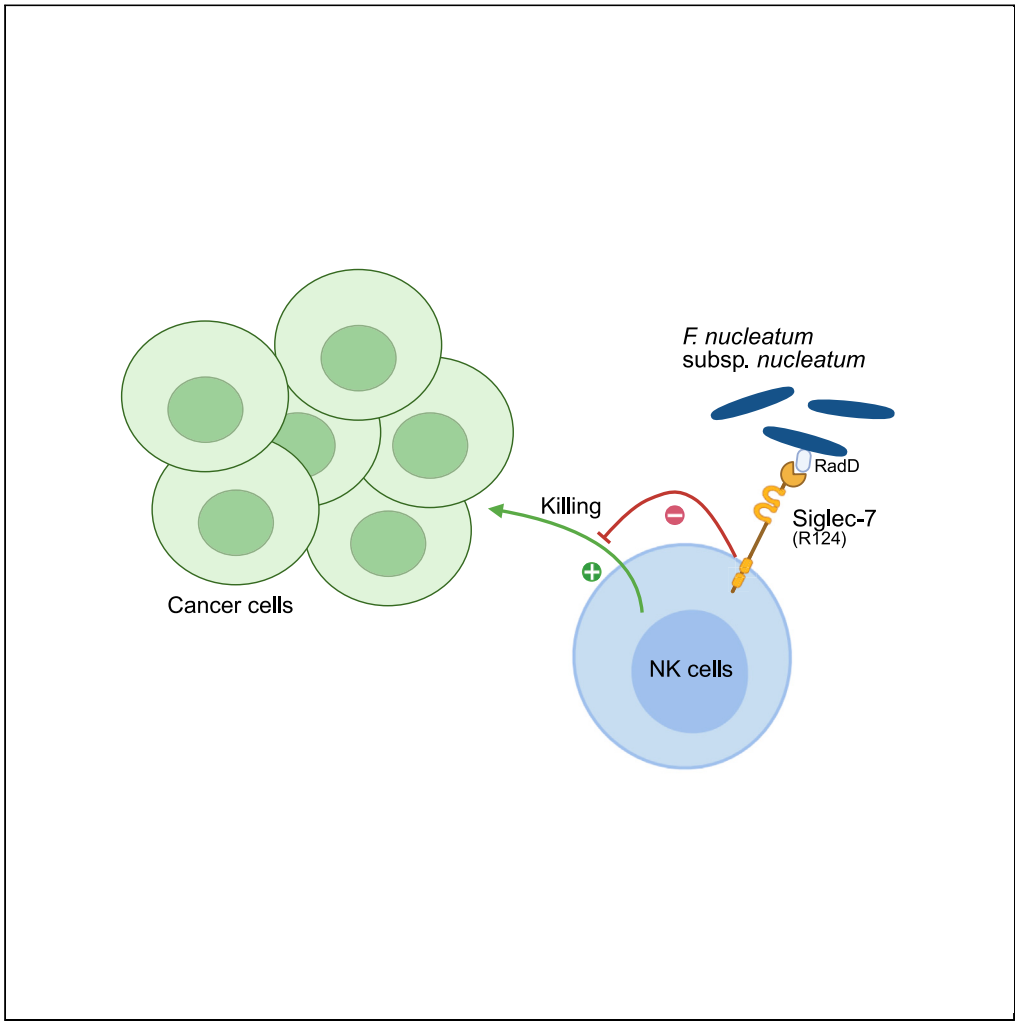

Johanna Galaski, Ahmed Rishiq, Mingdong Liu, ..., Renate Lux, Gilad Bachrach, Ofer Mandelboim

oferm@ekmd.huji.ac.il

Highlights

F. nucleatum 23726 inhibits NK cell-mediated cancer cell killing via Siglec-7

The *F. nucleatum* 23726 autotransporter RadD is the bacterial ligand of Siglec-7

Binding is dependent on arginine residue R124 in Siglec-7

Galaski et al., iScience 27, 110157
June 21, 2024
https://doi.org/10.1016/j.isci.2024.110157

iScience

CellPress
OPEN ACCESS

Article

Fusobacterium nucleatum subsp. *nucleatum* RadD binds Siglec-7 and inhibits NK cell-mediated cancer cell killing

Johanna Galaski,[1,2,3] Ahmed Rishiq,[1] Mingdong Liu,[1] Reem Bsoul,[4] Almog Bergson,[1] Renate Lux,[5] Gilad Bachrach,[4,6] and Ofer Mandelboim[1,6,7,*]

SUMMARY

***Fusobacterium nucleatum* is an oral commensal bacterium that can colonize extraoral tumor entities, such as colorectal cancer and breast cancer. Recent studies revealed its ability to modulate the immune response in the tumor microenvironment (TME), promoting cancer progression and metastasis. Importantly, *F. nucleatum* subsp. *animalis* was shown to bind to Siglec-7 via lipopolysaccharides, leading to a pro-inflammatory profile in human monocyte-derived dendritic cells. In this study, we show that *F. nucleatum* subsp. *nucleatum* RadD binds to Siglec-7 on NK cells, thereby inhibiting NK cell-mediated cancer cell killing. We demonstrate that this binding is dependent on arginine residue R124 in Siglec-7. Finally, we determine that this binding is independent of the known interaction of RadD with IgA. Taken together, our findings elucidate the targeting of Siglec-7 by *F. nucleatum* subsp. *nucleatum* RadD as a means to modulate the NK cell response and potentially promoting immune evasion and tumor progression.**

INTRODUCTION

The interplay between cancer cells and immune cells within the tumor microenvironment (TME) shapes tumor progression, metastasis, and therapeutic outcomes. In recent years, the importance of tumor-resident bacteria has become increasingly evident. Landmark studies have revealed that the tumor microbiome is tumor-type specific[1] and organized in specific microniches, influencing cancer progression and immune responses.[2] In this context, the commensal bacterium *Fusobacterium nucleatum* has emerged as a prominent player due to its association with various malignancies including colorectal,[3] esophageal,[4] pancreatic,[5] and breast cancer.[6] Mounting evidence suggests that *F. nucleatum* can manipulate the immune response, contributing to an immunosuppressive environment. More specifically, we previously showed that *F. nucleatum* engages the inhibitory immune receptor T cell immunoreceptor with Ig and immunoreceptor tyrosine-based inhibitory motif (ITIM) domains (TIGIT), expressed on NK and T cells, via its adhesion protein Fap2.[7] Furthermore, we and others found that *F. nucleatum* targets the inhibitory receptor carcinoembryonic antigen cell adhesion molecule 1 (CEACAM1) via the CEACAM binding protein of *Fusobacterium* (CbpF),[8,9] leading to T cell inhibition.[10] Here, we show that *F. nucleatum* subsp. *nucleatum* binds to the inhibitory receptor Siglec-7 via its major adhesin RadD and protects cancer cells from natural killer (NK) cell cytotoxicity.

Siglec-7 is a member of the sialic acid-binding immunoglobulin-like lectins (Siglecs) that is predominantly expressed on NK cells. It recognizes sialic acid-containing glycans and regulates immune cell functions. Inhibitory signaling is mediated via cytosolic ITIMs. It was previously shown that Siglec-7 ligands are overexpressed on a broad range of human malignancies and that NK cell antitumor immunity is attenuated after engagement of Siglec-7 ligands.[11] Interestingly, several bacteria have convergently evolved ligands for Siglec-7. For instance, group B *streptococcus* (GBS) binds to Siglec-7 both through sialylated capsular polysaccharides[12] and via its cell wall-anchored β antigen in a sialic acid-independent manner.[13] In another study, Lamprinaki and colleagues showed for the first time that *F. nucleatum* ssp. *animalis* binds to Siglec-7. The interaction was observed using whole bacteria, *F. nucleatum*-derived outer membrane vesicle and lipopolysaccharide (LPS). Intriguingly, this led to a pro-inflammatory profile in human monocyte-derived dendritic cells.[14]

In this study, we demonstrate the direct binding between *F. nucleatum* subsp. *nucleatum* RadD and Siglec-7, leading to an inhibition of NK cell killing of tumor cells. We further show that this interaction depends on arginine residue R124 in Siglec-7. Taken together, *F. nucleatum*

[1]The Concern Foundation Laboratories at the Lautenberg Center for General and Tumor Immunology, Department of Immunology and Cancer Research, Institute for Medical Research Israel Canada (IMRIC), Faculty of Medicine, The Hebrew University Medical School, Jerusalem, Israel
[2]I. Department of Medicine, University Medical Center Hamburg-Eppendorf, Hamburg, Germany
[3]Institute of Medical Microbiology and Hygiene, Medical Centre University of Freiburg, Freiburg, Germany
[4]The Institute of Dental Sciences, The Hebrew University-Hadassah School of Dental Medicine, Jerusalem, Israel
[5]Section of Periodontics, Division of Constitutive & Regenerative Sciences, UCLA School of Dentistry, Los Angeles, CA 90095, USA
[6]These authors contributed equally
[7]Lead contact
*Correspondence: oferm@ekmd.huji.ac.il
https://doi.org/10.1016/j.isci.2024.110157

subsp. *nucleatum* RadD may exploit Siglec-7 as a means to modulate NK cell responses within the TME, consequently promoting immune evasion and facilitating tumor progression.

RESULTS

F. nucleatum subsp. *nucleatum* binds Siglec-7

F. nucleatum subp. *nucleatum* is known to bind to several immune receptors such as CEACAM1 and TIGIT to circumvent the immune response.[7–10] Here, we assessed binding of FITC-labeled *F. nucleatum* subsp. *nucleatum* strain ATCC 23726 (subsequently abbreviated as *Fnn* 23726) to several different NK cell receptor fusion proteins in which the extracellular domain of the respective immune receptor is fused to the Fc portion of human IgG1 (containing the N297A mutation to abrogate Fc receptor binding). We found that *Fnn* 23726 binds to Siglec-7-Ig, but not NTB-A-Ig, 2B4-Ig, and CD16-Ig (Figures 1A and S1 with gating strategy). To elucidate whether interaction with Siglec-7 is a conserved feature among different *F. nucleatum* subspecies, we evaluated additional strains of the *F. nucleatum* subspecies *nucleatum* and *polymorphum* (Figure 1B). While *Fnn* 23726 and *Fnn* 25586 both bound to Siglec-7-Ig, *F. nucleatum* subsp. *polymorphum* strains ATCC 10953 and 12230 (subsequently abbreviated as *Fnp* 10953 and *Fnp* 12230) showed little to no staining.

Finally, we also tested *F. nucleatum* strain CTI-7, a clinical isolate recovered from human colon adenocarcinoma, which lacks the autotransporter protein Fap2.[7] Clinical isolate CTI-7 consistently showed binding to Siglec-7-Ig (Figure 1C).

F. nucleatum subspecies *nucleatum* leads to Siglec-7-dependent inhibition of NK cell-mediated cancer cell killing

Next, we wanted to assess the effect of *F. nucleatum* binding to Siglec-7 on NK cell killing of cancer cells using *Fnn* 23726 as a representative strain. However, *F. nucleatum* interacts with several NK cell receptors, hindering our ability to directly investigate the binding of *F. nucleatum* to Siglec-7 on NK cells. Consequently, we established a controlled experimental system to isolate the effect of *F. nucleatum* binding to Siglec-7. The NK cell line YTS Eco does not express any known inhibitory NK cell receptors and activation of this cell line is mainly dependent on the engagement of the activating receptor 2B4 by CD48.[15] *Fnn* 23726 does not bind to 2B4 Ig (Figure 1A), which makes this cell line ideal for testing the effect of the interaction of *Fnn* 23726 and Siglec-7 on NK cell cytotoxicity. We established YTS Eco cell lines using the lentiviral vector pHage-DsRED(−)-eGFP(+) (empty vector; EV) or the vector containing the human *siglec-7* gene. We then conducted binding assays between *Fnn* 23726 and YTS Siglec-7 cells before sorting. This allowed us to directly compare binding of *Fnn* 23726 to YTS cells that expressed no to low levels of Siglec-7 and YTS cells that expressed high levels of Siglec-7. We used GFP as a surrogate for Siglec-7 expression (Figure S2A). We found that binding of Cy5-labeled *Fnn* 23726 to YTS cells expressing high levels of Siglec-7 was significantly higher compared to YTS cells expressing no to low levels of Siglec-7 ($p < 0.0001$; Figures S2B and S2C), suggesting that *Fnn* 23726 binds to Siglec-7 expressed on YTS cells. However, the effects were only subtle, since Siglec-7 is only one of many cell surface receptors that *Fnn* 23726 is known to interact with.

Next, we assessed the cytotoxicity of YTS empty vector (EV) or YTS Siglec-7 cells toward the CD48-positive target cells 721.221 and BCBL1 in the presence or absence of *Fnn* 23726 (illustrated in Figure 2A). Levels of the activating receptor 2B4 were comparable in both YTS EV and YTS Siglec-7 cells (Figure 2B). Both target cell lines were found to express Siglec-7 ligands (Figures 2C and 2D). In the absence of Siglec-7, we observed no difference in 721.221 and BCBL1 cell killing with or without bacteria (Figures 2E and 2F). Consistent with the expression of Siglec-7 ligands on both cell lines, killing of 721.221 and BCBL1 cells by YTS Siglec-7 cells in the absence of *Fnn* 23726 was significantly reduced in comparison to YTS EV cells ($p = 0.029$ and $p = 0.036$, respectively) (Figures 2E and 2F). No relevant cell death was observed for YTS EV or YTS Siglec-7 cells following incubation with cancer cell lines (Figure S3). Importantly, in the presence of *Fnn* 23726, killing of both 721.221 and BCBL1 cells by YTS Siglec-7 cells was significantly inhibited ($p = 0.034$ and $p = 0.044$, respectively) (Figures 2E and 2F). Taken together, these results indicate that binding of *Fnn* 23726 to Siglec-7 inhibits NK cell cytotoxicity toward cancer cells.

The *Fnn* 23726 autotransporter RadD is the bacterial ligand of Siglec-7

To elucidate the nature of the ligand of Siglec-7 in *Fnn* 23726, we immunoprecipitated bacterial lysates with Siglec-7-Ig or controls. Visualization of immunoprecipitates revealed a large band (>250 kDa) that was identified as *Fnn* 23726 RadD by mass spectrometry (Figure 3A). This band was not present in the negative control (Figure 3A). As a positive control we used CEACAM1-Ig that yielded a band of the size of its known binding partner *Fnn* 23726 CbpF.[8] This band did not appear for the mutant ΔN CEACAM1-Ig that does not interact with CbpF (Figure 3A).[8,10] Additional bands either matched the size of the fusion proteins used for immunoprecipitation or were unspecific. To corroborate *Fnn* 23726 RadD as the ligand of Siglec-7, we repeated the immunoprecipitation using lysates of a ΔRadD *Fnn* 23726 mutant. As expected, the band that was immunoprecipitated with Siglec-7-Ig using wild-type *Fnn* 23726 was not detected, while binding of CEACAM1-Ig to CbpF was still retained (Figure 3B). Consistent with these findings, when the *Fnn* 23726 ΔRadD mutant was incubated with Siglec-7-Ig and analyzed using flow cytometry, it exhibited a total loss of binding. In contrast, the wild-type counterpart displayed staining with Siglec-7-Ig (Figures 3C, quantified in 3D). We thus identified RadD as the *Fnn* 23726 ligand for Siglec-7.

Importantly, RadD is known to be expressed in *Fnn* 23726, *Fnn* 25586, and *Fnp* 10953.[16,17] Analysis of the *Fnp* 12230 genome (accession number gb|CP053468.1) revealed that it encodes eight open reading frames that are annotated as autotransporter or fdes (Table S1). Of these, only five contain the beta-barrel that is characteristic for large autotransporter-like outer membrane proteins like RadD. None of the *Fnp* 12230 proteins is similar in length (Table S1) or exhibits a close phylogenic relationship to RadD of *Fnn* 23726, *Fnn* 25586, or *Fnp* 10953 (Figure S4). Consistent with the absence of a RadD homolog in *Fnp* 12230, this strain showed no binding to Siglec-7 (Figure 1).

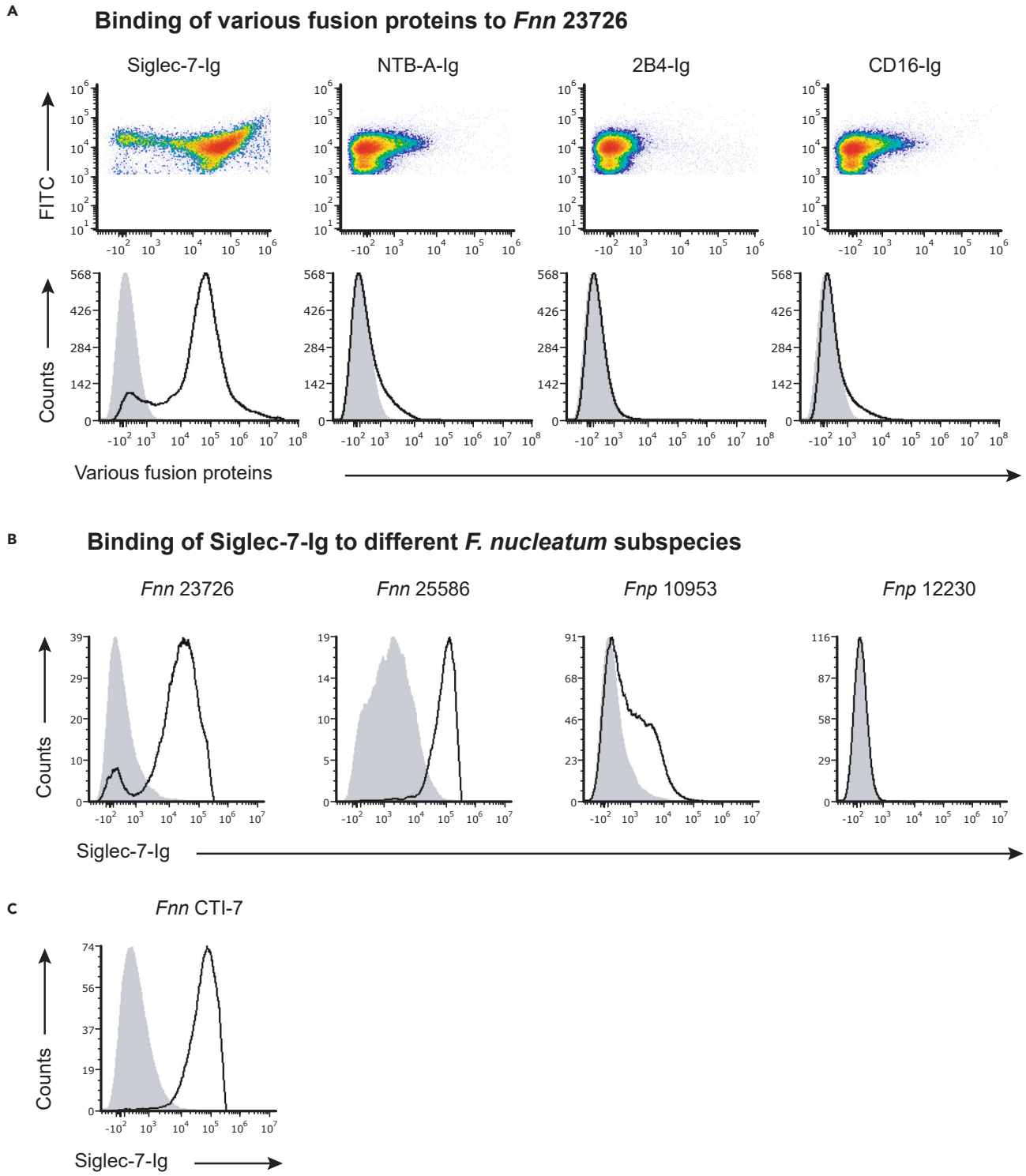

Figure 1. Siglec-7 binding to *F. nucleatum* strains

(A) FITC-labeled *F. nucleatum* subsp. *nucleatum* ATCC 23726 (*Fnn* 23726) was incubated with 2 μg of Siglec-7-Ig, NTB-A-Ig, 2B4-Ig, or CD16-Ig and binding was revealed with fluorescently labeled secondary antibodies. Filled gray histograms represent staining with secondary antibody only. One representative experiment out of three is shown.

(B) Two strains of *F. nucleatum* subsp. *nucleatum* (*Fnn* 23726 and *Fnn* 25586) and two strains of *F. nucleatum* subsp. *polymorphum* (*Fnp* 10953 and *Fnp* 12230) as well as (C) a clinical strain of *F. nucleatum* (*Fnn* CTI-7) were incubated with Siglec-7-Ig. Filled gray histograms represent staining with secondary antibody only. One representative experiment out of two is shown.

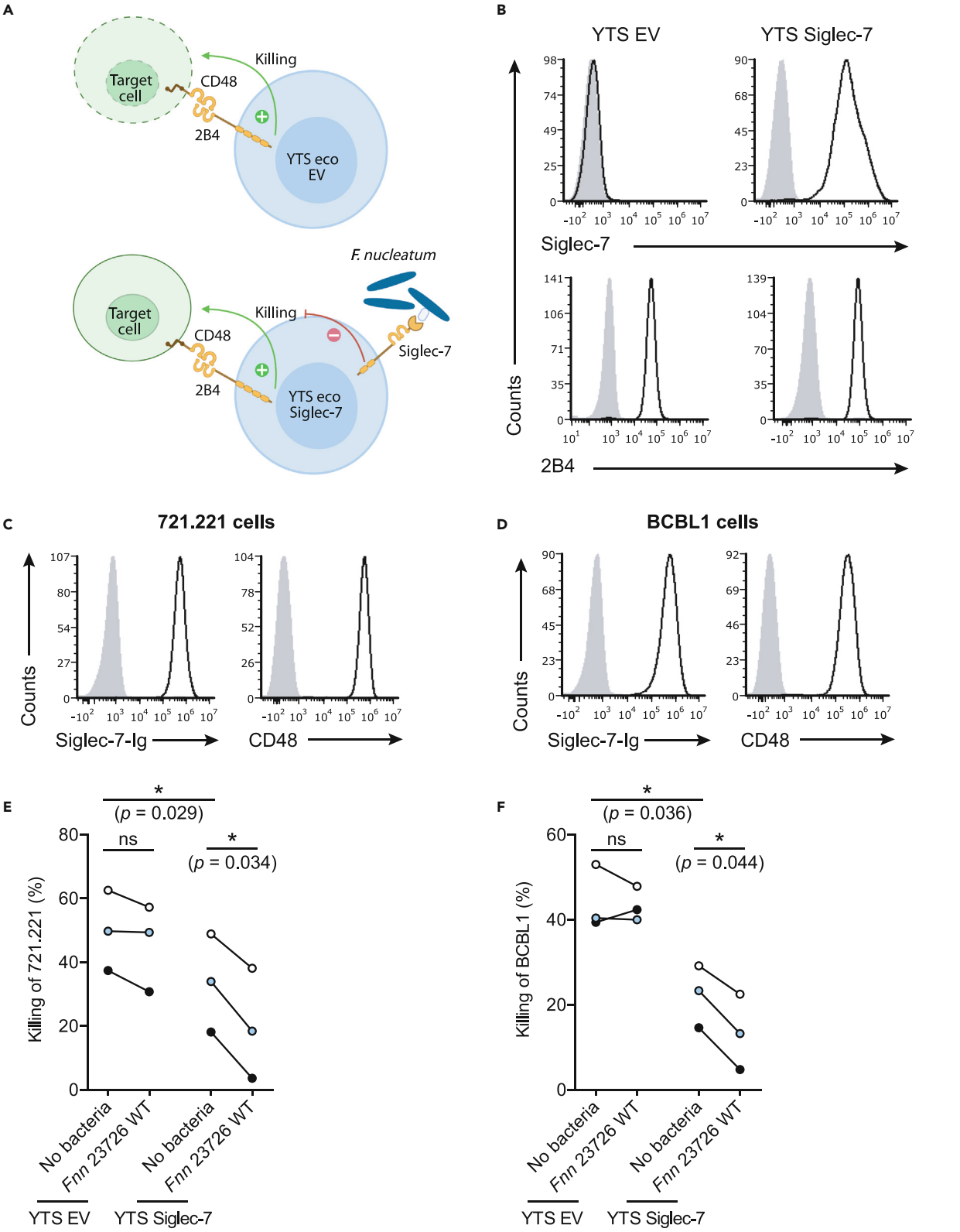
A
Target cell
CD48
2B4
Killing
YTS eco EV
F. nucleatum
Target cell
CD48
2B4
Killing
Siglec-7
YTS eco Siglec-7
B
YTS EV
YTS Siglec-7
Siglec-7
Counts
2B4
C
721.221 cells
Counts
Siglec-7-Ig
CD48
D
BCBL1 cells
Counts
Siglec-7-Ig
CD48
E
(p = 0.029)
ns
(p = 0.034)
Killing of 721.221 (%)
No bacteria
Fnn 23726 WT
No bacteria
Fnn 23726 WT
YTS EV
YTS Siglec-7
F
(p = 0.036)
ns
(p = 0.044)
Killing of BCBL1 (%)
No bacteria
Fnn 23726 WT
No bacteria
Fnn 23726 WT
YTS EV
YTS Siglec-7

Figure 2. *F. nucleatum* subsp. *nucleatum* confers Siglec-7-dependent protection against NK cell-mediated cancer cell killing

(A) Schematic representation of target cell killing by YTS EV or YTS Siglec-7 cells. YTS empty vector (EV) or YTS Siglec-7 cells are activated almost exclusively by CD48-expressing target cells via their activating receptor 2B4. In the presence of bacteria, killing of target cells is inhibited via Siglec-7.

(B) Staining of YTS EV or YTS Siglec-7 cells with Siglec-7 (upper histograms) and 2B4 (lower histograms) antibodies. Filled gray histograms represent staining with isotype control and secondary antibody only, respectively.

(C) Staining of 721.221 or (D) BCBL-1 cells for Siglec-7 ligands with Siglec-7-Ig or of CD48 expression using anti-CD48 antibodies. (E) YTS EV or YTS Siglec-7 cells were precincubated or not with *F. nucleatum* subsp. *nucleatum* ATCC 23726 (*Fnn* 23726) at a ratio of 1:20 for 30 min at 37°C. The cells were then incubated with Calcein AM-labeled 721.221 or (F) BCBL-1 cells at an E:T ratio of 10:1 for 4 h at 37°C and the Calcein release into the supernatant was quantified. Each graph shows data from three independent experiments and each independent experiment is colored differently (white, blue, and black). Each experiment was performed in triplicates. Significance was tested using mixed-effects analysis with the Geisser-Greenhouse correction and Sidak's multiple comparisons test (* $p \leq 0.05$; ** $p \leq 0.01$; *** $p \leq 0.001$).

Binding of RadD to Siglec-7 is blocked by arginine and lysine

Previous research demonstrated the inhibitory effect of arginine on *F. nucleatum* RadD interactions.[16] This prompted us to investigate whether arginine impacts the interaction between *Fnn* 23726 RadD and Siglec-7. Indeed, binding of *Fnn* 23726 to Siglec-7-Ig was sensitive to increasing concentrations of arginine (Figure 4A). More specifically, at a concentration of only 5 mM, binding to Siglec-7-Ig was already reduced by 31% ($p < 0.0001$) (Figure 4B). In contrast, binding of CEACAM1-Ig was not reduced in the presence of arginine (Figures 4C, quantified in 4D).

More recently, lysine, another positively charged amino acid, was shown to inhibit RadD-dependent coaggregation.[18] Similar to our experiments with arginine, we conducted blocking experiments to assess the effect of lysine on the binding of *Fnn* 23726 to Siglec-7-Ig. Consistently, we found that the binding of *Fnn* 23726 to Siglec-7-Ig was impaired by lysine in a dose-dependent manner (Figure S5). Conversely, no such effect was observed for the binding of *F. nucleatum* to Ceacam1-Ig. These findings reveal the inhibitory effect of arginine and lysine on the RadD-Siglec-7 interaction.

Binding of RadD to Siglec-7 is dependent on the arginine residue R124 in Siglec-7 and can be blocked using the Siglec-7 antibody S7.7

A previous study that resolved the high-resolution crystal structure of Siglec-7 found that arginine R124 is a key residue. It interacts with sialic acids and is thus pivotal for sialic acid-dependent ligand binding.[19] Binding of a Siglec-7 R124A-Ig mutant to ligands such as gangliosides GM3, GD3, GD1a, and GT1b as well as leukosialin (CD43) was previously shown to be disrupted.[20,21] De-sialylation of *Fnn* 23726 did not affect binding to Siglec-7 (Figure S6), in line with the lack of *de novo* synthesis of sialic acids in this strain.[22] However, RadD is known to bind to arginine[17] and we thus hypothesized that arginine R124 might be critical for RadD binding to Siglec-7. To test this hypothesis, we generated a Siglec-7 R124A-Ig mutant. The fusion protein Siglec-7 R124A-Ig was detected by Siglec-7-specific antibodies at similar levels as the wild-type protein (data not shown), consistent with previous findings,[23] indicating that it is stably expressed. Strikingly, binding of Siglec-7 R124A-Ig to *Fnn* 23726 was comparable to background levels (Figures 4E, quantified in 4F). In line with these results, Siglec-7 R124A-Ig failed to efficiently precipitate RadD (Figure 4G).

Next, we sought to investigate whether the interaction between *Fnn* 23726 and Siglec-7 could be blocked using Siglec-7 antibodies. When Siglec-7-Ig was pre-incubated with the Siglec-7 monoclonal antibody S7.7, binding to *Fnn* 23726 was almost reduced to background levels (Figure S7). In contrast, binding was unaffected by Siglec-7 antibody K8 (data not shown). Subsequent attempts to use Siglec-7 antibody S7.7 for blocking in functional experiments were inconclusive, due to the functional inhibition of the NK cell response by the antibody. In line with these results, previous studies found this antibody to cross-link and functionally suppress NK cell activity.[13,24] Taken together, these findings highlight the importance of Siglec-7 arginine residue R124 and identify Siglec-7 antibody S7.7 as a blocking antibody for the interaction between *Fnn* 23726 and Siglec-7.

Binding of Siglec-7 to RadD on different binding site compared to IgA

RadD (previously referred to as high molecular weight arginine-binding protein) of *Fnp* 10953 was previously shown to bind to secretory IgA.[17] Intriguingly, GBS β antigen was shown to bind to Siglec-7 via its B6N segment[13] and to IgA via the adjacent IgA-binding region (IgA-BR).[25] To gain a broader understanding of RadD-dependent immune evasion strategies and recognition of Siglec-7, we were interested to test whether the *Fnn* 23726 also binds to human IgA and whether this binding competes with binding to Siglec-7. We thus incubated both *Fnn* 23726 and its ΔRadD mutant derivative with increasing amounts of human IgA. We found that the wild-type strain bound IgA in a concentration-dependent manner (Figures 5A and 5C) while the ΔRadD strain showed weaker binding (Figures 5B and 5D), indicating that *Fnn* 23726 RadD is involved in binding IgA but that other fusobacterial proteins may also contribute to the interaction (Figures 5A–5D). Next, we performed a competition assay by preincubating *Fnn* 23726 with increasing amounts of IgA to saturate binding sites before staining with Siglec-7-Ig. We observed no concentration-dependent decrease in the binding of Siglec-7-Ig to RadD, indicating that IgA and Siglec-7 may have distinct binding sites on RadD (Figures 5E, quantified in 5F).

DISCUSSION

The presence of *F. nucleatum* within the TME of several cancer entities has been associated with tumor progression, metastasis, and immune evasion.[2,6,26] In this study, we show that RadD of *F. nucleatum* subsp. *nucleatum* binds to the inhibitory immune receptor Siglec-7, adding to previously established immune inhibitory interactions including the binding of Fap2 to TIGIT[7] and CbpF to CEACAM1.[8,9]

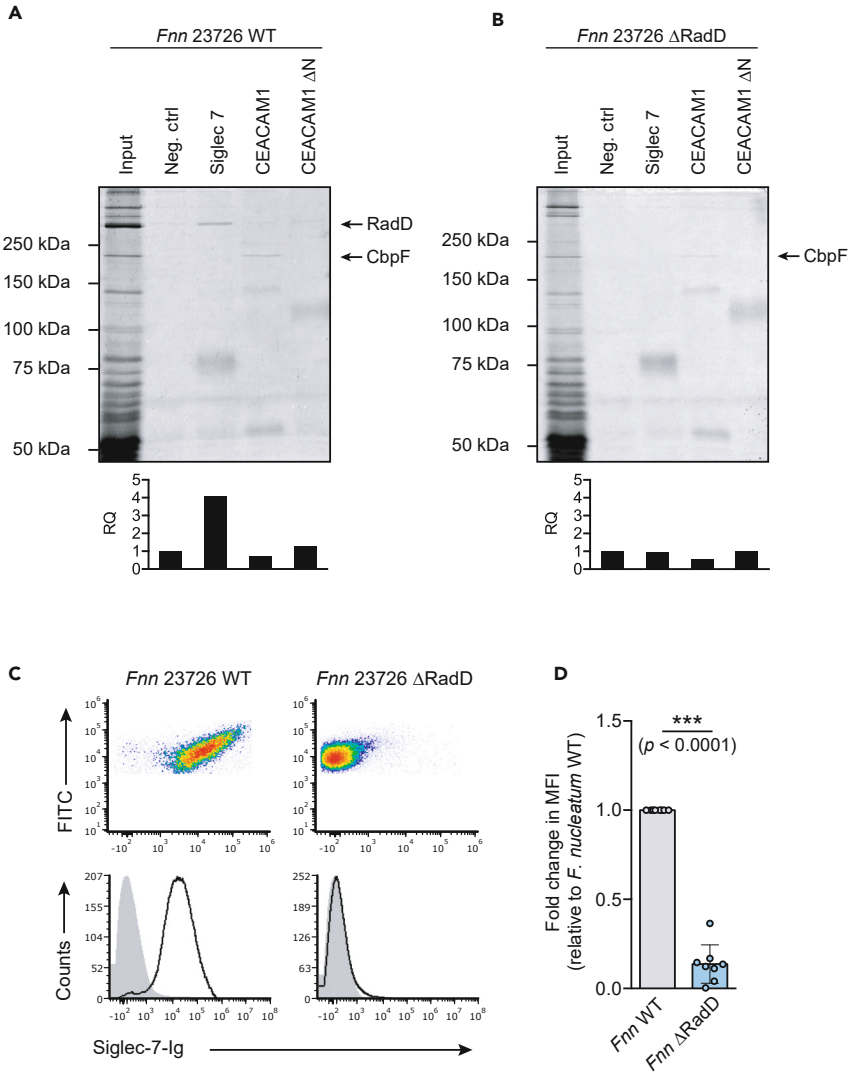

Figure 3. RadD of *F. nucleatum* subsp. *nucleatum* is the bacterial ligand for Siglec-7

Lysates prepared from (A) *F. nucleatum* subsp. *nucleatum* ATCC 23726 WT (*Fnn* 23726 WT) or (B) *F. nucleatum* subsp. *nucleatum* ATCC 23726 ΔRadD (*Fnn* 23726 ΔRadD) were immunoprecipitated using Siglec-7-Ig, CEACAM1-Ig, or CEACAM1 ΔN-Ig. Immunoprecipitates were visualized by Coomassie blue and immunoprecipitated bands were analyzed by mass spectrometry. RadD levels were quantified relative to the negative control. RQ, relative quantification.

(C) FITC-labeled *Fnn* 23726 WT or its ΔRadD mutant was stained with Siglec-7-Ig. Filled gray histograms represent staining with secondary antibody only. One representative experiment out of eight is shown.

(D) Quantification of Siglec-7-Ig binding to *Fnn* 23726 WT and the ΔRadD mutant shown as fold change in median fluorescent intensity (MFI) relative to *Fnn* 23726 WT. Bars represent means of eight independent experiments. Statistical significance was assessed using a two-tailed unpaired t test (* $p \leq 0.05$; ** $p \leq 0.01$; *** $p \leq 0.001$).

The diversification of immune evasion mechanisms provides several potential benefits. First, by engaging different immune inhibitory receptors, inhibition of the immune response is amplified and an immunosuppressive environment is sustained. Moreover, it allows for the engagement of different immune cell subsets with heterogeneous expression patterns of inhibitory receptors: while TIGIT is expressed on both T and NK cells,[27]; CEACAM1 is predominantly expressed on activated T cells,[28] and Siglec-7 is expressed on a major subset of NK cells.[29] Finally, some *F. nucleatum* strains only express a subset of virulence factors. For instance, CTI-7 used in this study expresses RadD but not Fap2. A comprehensive study published in Nature sheds light on the genetic variability in key virulence factors among *Fusobacterium* species.[30] Specifically, the study reveals that while F. *nucleatum* subsp. *nucleatum* strains often possess both the genes for *radD* and *fap2*, F. *nucleatum* subsp. *animalis* strains frequently harbor either one or the other. This genetic variability underscores the adaptability of *Fusobacterium* species in modulating immune responses and the advantage of targeting tumor surveillance via multiple pathways.

Previous studies have shown that Siglec-7 ligands are overexpressed on several different cancer cell types and inhibit the NK cells response.[11,31] Indeed, the target cell lines used in this study to assess NK cell killing in the presence or absence of *F. nucleatum* expressed

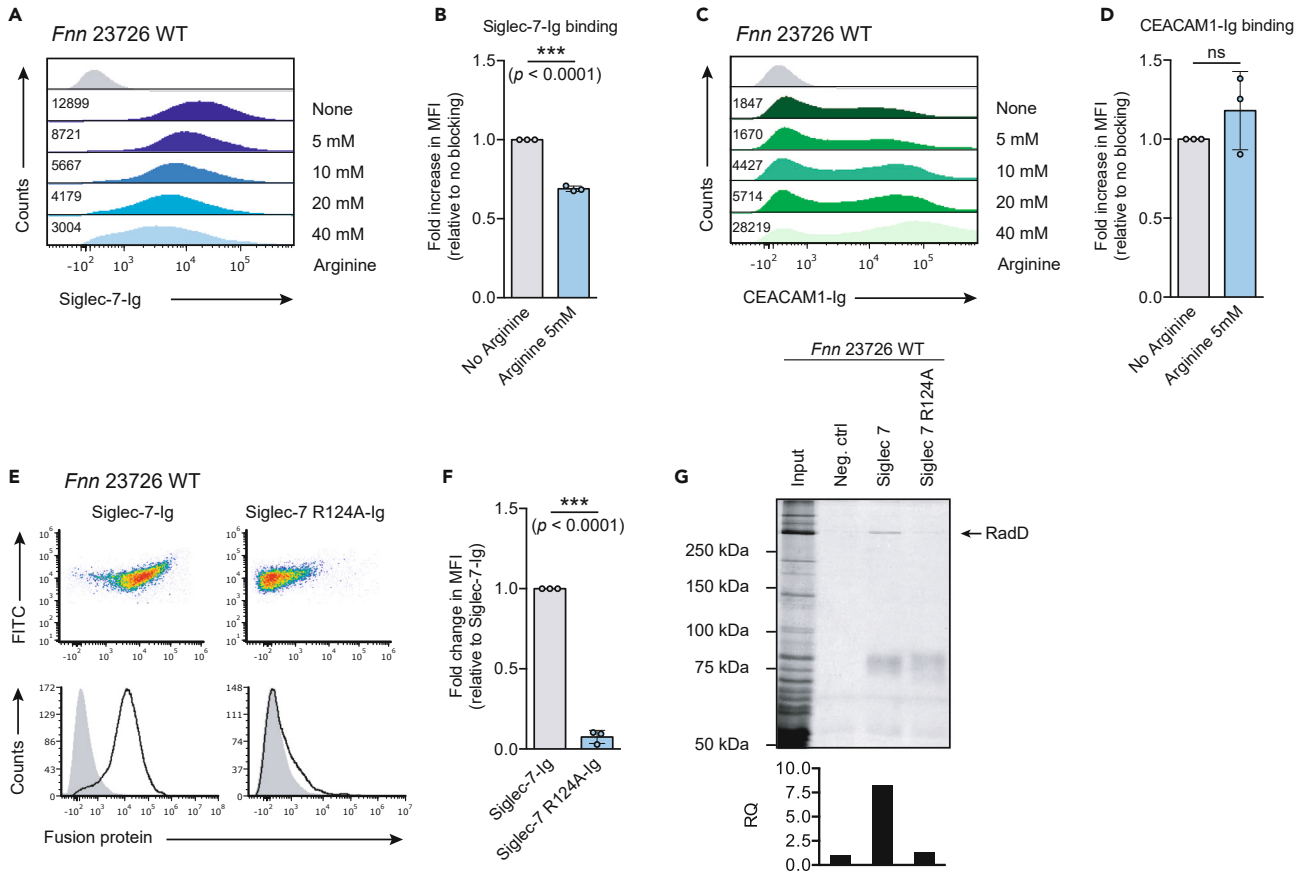

Figure 4. RadD binding to Siglec-7 is inhibited by arginine and dependent on Siglec-7 arginine residue R124

(A) Staining of *Fnn* 23726 WT with Siglec-7-Ig or (C) CEACAM1-Ig in the presence of increasing concentrations of arginine. Filled gray histograms represent staining with secondary antibody only. MFI values are indicated left of each histogram.

(B) Quantification of three independent experiments showing binding of Siglec-7-Ig or (D) CEACAM1-Ig as fold change in MFI in the presence of 5 mM arginine relative to no blocking. Statistical significance was assessed using a two-tailed unpaired Student's t test (* $p \leq 0.05$; ** $p \leq 0.01$; *** $p \leq 0.001$).

(E) FITC-labeled *Fnn* 23726 WT were stained with Siglec-7-Ig or Siglec-7 R124A-Ig. Filled gray histograms represent staining with secondary antibody only. One representative staining out of three is shown.

(F) Siglec-7-Ig and Siglec-7 R124A-Ig staining of *Fnn* 23726 WT quantified and shown as fold change in MFI relative to staining with Siglec-7 Ig. Bars represent means of three independent experiments. Statistical significance was assessed using a two-tailed unpaired Student's t test (* $p \leq 0.05$; ** $p \leq 0.01$; *** $p \leq 0.001$).

(G) Lysates prepared from *Fnn* 23726 WT were immunoprecipitated using Siglec-7-Ig or Siglec-7 R124A-Ig. Immunoprecipitates were visualized by Coomassie. RadD levels were quantified relative to the negative control. RQ, relative quantification.

high levels of Siglec-7 ligands. While expression of Siglec-7 ligands in these cell lines conferred protection from NK cell cytotoxicity, this effect was amplified in the presence of bacteria. Of note, several colorectal cancer and breast cancer cell lines—tumor entities where *F. nucleatum* is frequently enriched—express little to no Siglec-7 ligands.[11,31]

The ability of RadD to recognize Siglec-7 seems to be dependent on the fusobacterial subspecies. While Siglec-7 showed strong binding to *F. nucleatum* subsp. *nucleatum*, little to no binding was observed for *F. nucleatum* subsp. *polymorphum*. For *Fnp* 12230, the lack of binding is explained by the absence of a RadD protein in this strain. The observed residual binding of *Fnp* 10953 may be attributed to its expression of sialic acids,[22] as a mutant of *Fnp* 10953 lacking RadD still maintained the same low binding to Siglec-7 (data not shown), further suggesting that this interaction might be mediated by sialylated surface glycans and not by RadD. Interestingly, previous work showed that RadD of *F. nucleatum* subsp. *nucleatum* and *polymorphum* differ in the adhesins they recognize on *Streptococcus mutans*,[32] highlighting their distinct binding characteristics. Differences in the amino acid sequence of RadD from strains *F. nucleatum* 23726 and *F. polymorphum* 10953, which share only 68.5% homology, might inform future studies aiming at deciphering the RadD domains involved in Siglec-7 binding.

Several bacteria have previously been reported to bind to Siglecs through surface glycans, such as *Campylobacter jejuni* sialylated lipooligosaccharides,[33] *Neisseria meningitides* sialylated lipopolysaccharides,[34] and GBS capsular sialic acids.[12] Notably, an independent study reported binding of *F. nucleatum* subsp. *animalis* to Siglec-7 and demonstrated that LPS glucosaminuronic and fusosamine residues interacted with Siglec-7, consistent with the absence of sialic acids in the strain studied.[14] Here, we identified the autotransporter RadD of

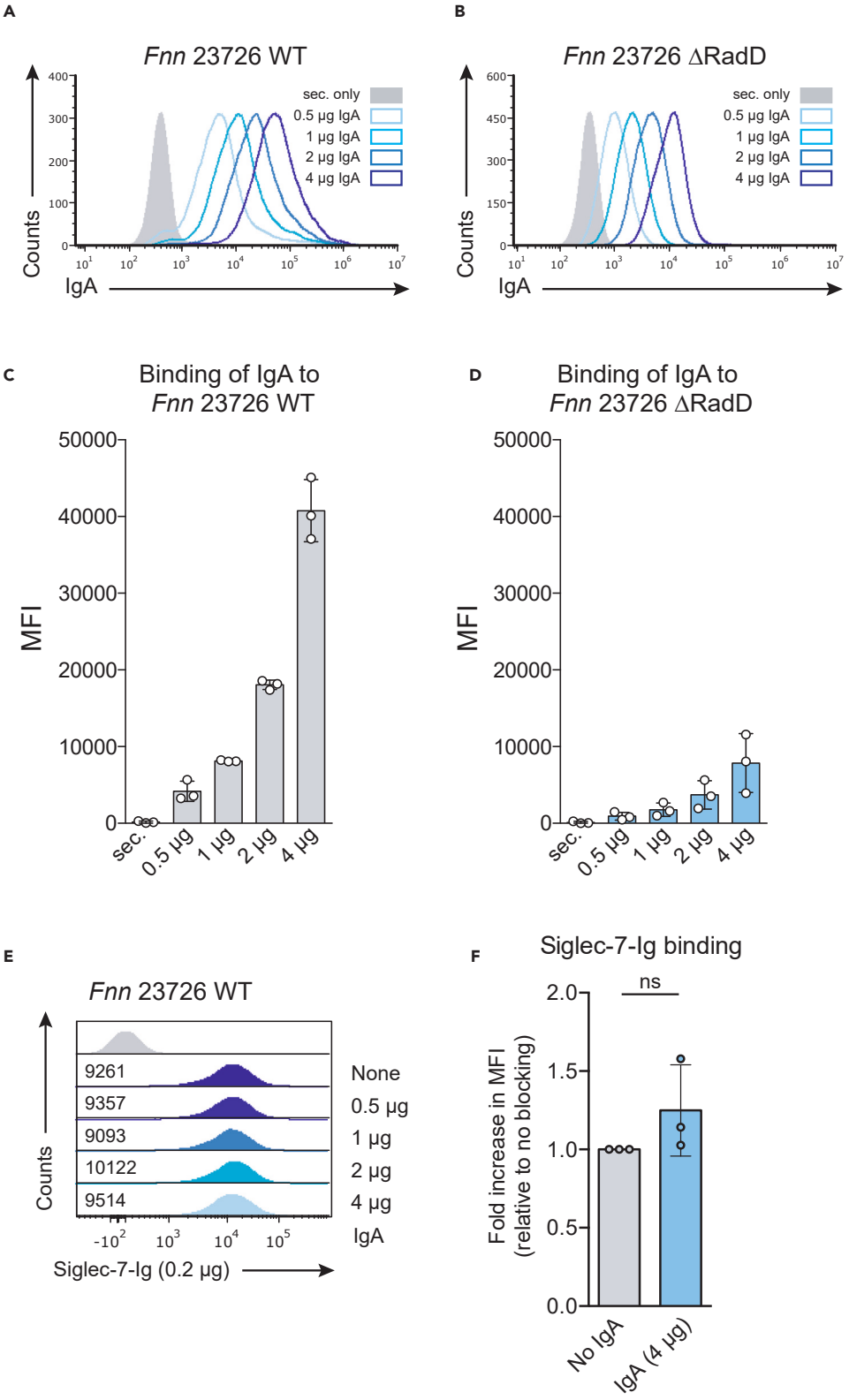
A
Fnn 23726 WT
sec. only
0.5 µg IgA
1 µg IgA
2 µg IgA
4 µg IgA
Counts
IgA
B
Fnn 23726 ΔRadD
C
Binding of IgA to
Fnn 23726 WT
MFI
sec.
0.5 µg
1 µg
2 µg
4 µg
D
Binding of IgA to
Fnn 23726 ΔRadD
E
Fnn 23726 WT
9261
9357
9093
10122
9514
None
0.5 µg
1 µg
2 µg
4 µg
IgA
Siglec-7-Ig (0.2 µg)
F
Siglec-7-Ig binding
ns
Fold increase in MFI
(relative to no blocking)
No IgA
IgA (4 µg)

Figure 5. IgA does not block binding of Siglec-7-Ig to *F. nucleatum*

(A) FITC-labeled *Fnn* 23726 WT or (B) *Fnn* 23726 ΔRadD were stained with increasing amounts of human serum IgA (0.5 μg, 1 μg, 2 μg, and 4 μg). Filled gray histograms represent staining with secondary antibody only. One representative experiment out of three is shown. Quantification of the MFI of three independent stainings of (C) *Fnn* 23726 WT and (D) *Fnn* 23726 ΔRadD with human serum IgA is shown.

(E) Staining of *F. nucleatum 23726* WT with Siglec-7-Ig after preincubation of bacteria with increasing amounts of human serum IgA. Filled gray histograms represent staining with secondary antibody only. MFI values are indicated left of each histogram.

(F) Quantification of three independent experiments showing the fold increase in MFI in the presence of 4 μg IgA relative to no blocking. Significance was tested using Student's t test (two-tailed and unpaired).

F. nucleatum subsp. *nucleatum 23726* as a ligand for Siglec-7. Whether LPS also contributes to Siglec-7 binding in *Fnn* 23726 was not investigated. However, a *Fnn* 23726 mutant strain lacking RadD showed no residual binding to Siglec-7, suggesting that RadD is the primary ligand of Siglec-7 in this strain and that LPS likely plays a minor role, if any.

RadD is an outer membrane adhesion protein that mediates coaggregation with other pathogens such as *Clostridium difficile*,[35] *Streptococcus mutans*,[32] and *Candida albicans*.[36] RadD was previously demonstrated to bind to arginine[16,17] and lysine.[18] The finding that coaggregation with other bacteria mediated by RadD can be effectively inhibited in the presence of arginine led to the nomenclature RadD or arginine (R)-inhibitable adhesin D.[16] We investigated the impact of arginine and lysine on the RadD-Siglec-7 interaction. We observed that both arginine and lysine indeed block the binding of RadD to Siglec-7. Furthermore, the mutation of the arginine residue R124, known for its role in forming a salt bridge with sialic acids and being crucial for sialic acid binding in all Siglecs (Angata et al., 2000), disrupted the RadD-Siglec-7 interaction. The binding of *F. nucleatum* RadD to exposed arginine residues likely enables promiscuous binding to a diverse range of host cells and bacteria. These binding characteristics might allow for a versatile strategy to engage multiple targets in the host and to manipulate the host immune system in a broad manner.

Edwards et al. demonstrated that a high molecular weight arginine-binding protein, now known as RadD, mediates binding of *F. nucleatum* to human secretory IgA, an interaction that was described in *Fnp* 10953.[17] Here, we show that *Fnn* 23726 binds to human serum IgA and that IgA and Siglec-7 likely interact with distinct binding sites on RadD. Remarkably, to the best of our knowledge, RadD represents the second bacterial protein, following GBS β antigen,[25] found to interact with both Siglec-7 and human IgA. Given that *F. nucleatum* RadD and GBS β antigen do not exhibit significant sequence homology, this suggests that both bacteria independently evolved the ability to interact with both Siglec-7 and human IgA, underscoring the potential significance of these distinct binding capabilities.

While our study did not explore RadD's role in *F. nucleatum* infection, a recent study investigated RadD in a mouse model of preterm birth associated with *F. nucleatum* infection using *Fnn* 23726.[18] Intriguingly, the study demonstrated that an *F. nucleatum* mutant lacking RadD displayed higher virulence, resulting in increased rates of preterm birth and elevated bacterial burden in maternal-fetal compartments. This contrasts with our finding that RadD binding to Siglec-7 inhibits the NK cell response. However, RadD has many functions and its role cannot be solely attributed to its interaction with Siglec-7. In addition, it's important to note that Siglec-7 doesn't have a counterpart in mice. To fully understand the impact of the RadD-Siglec-7 axis in infection, further studies using human Siglec-7 transgenic mice are needed.

In conclusion, we show that *F. nucleatum* subsp. *nucleatum* inhibits the NK cell antitumor response by manipulating the inhibitory receptor Siglec-7. We show that this binding is subspecies-dependent which may contribute to differential pathogenicity among fusobacterial subspecies. The RadD-Siglec-7 interaction adds to previously established inhibitory interactions between *F. nucleatum* and immune cell receptors, revealing both the complexity and the remarkable ingenuity of this pathogen in manipulating the host immune response.

Limitations of the study

While our study provides valuable insight into the role of *F. nucleatum* subsp. *nucleatum* in modulating the NK cell antitumor response via Siglec-7, it is important to acknowledge several limitations. Firstly, the complexity of the interplay between *F. nucleatum* and NK cells made it challenging to functionally study the interaction of *F. nucleatum* with Siglec-7. Thus, instead of primary NK cells, we relied on the YTS cell line as a surrogate. While this allowed us to focus on the functional consequences of Siglec-7 engagement, the reliance on a cell line model represents a potential limitation of our study, as it does not fully capture the complexities of NK cell biology and their interactions with *F. nucleatum*.

Secondly, we attempted functional experiments using the *F. nucleatum* ΔRadD mutant. However, due to the intricate involvement of RadD in various processes, including cell adhesion, functional experiments with the ΔRadD mutant did not yield conclusive results. This underscores the challenges in isolating the specific contribution of RadD-Siglec-7 binding to NK cell modulation.

Furthermore, while we identified Siglec-7 antibody S7.7 as a blocking antibody of the interaction between *Fnn* 23726 and Siglec-7, its application in functional experiments was hindered by the observed inhibitory signaling, consistent with existing literature.[13,24]

Lastly, we did not address whether blocking the interaction between RadD and Siglec-7 on NK cells would benefit the therapy of colorectal cancer or breast cancer *in vivo*. This aspect warrants further investigation in future studies.

STAR★METHODS

Detailed methods are provided in the online version of this paper and include the following:

- KEY RESOURCES TABLE
- RESOURCE AVAILABILITY
  - Lead contact

SUPPLEMENTAL INFORMATION

Supplemental information can be found online at https://doi.org/10.1016/j.isci.2024.110157.

ACKNOWLEDGMENTS

J.G. was supported by the German Research Foundation (DFG) with a postdoctoral research fellowship (project number 429842436). This work was supported by the Israel Science Foundation, Israel Precision Medicine Partnership program (grant No. 3042/22), the German-Israeli Foundation for Scientific Research and Development (grant No. 1412-414.13), the ICRF professorship grant, the Ministry of Science and Technology (grant No. 3-14764), and the MOST-DKFZ grant (grant No. 3-14931).

AUTHOR CONTRIBUTIONS

J.G. and O.M. conceived the study. J.G., A.R., M.L., R.B., and A.B. performed the experiments. J.G. and O.M. analyzed the data. R.L. contributed *F. nucleatum* mutants and analyses of *Fusobacterium* genomic information of autotransporter-like large outer membrane proteins. J.G. drafted the manuscript. O.M. and G.B. supervised the project. All authors revised and approved the manuscript.

DECLARATION OF INTERESTS

The authors declare no competing interests.

Received: November 10, 2023
Revised: April 23, 2024
Accepted: May 28, 2024
Published: May 31, 2024

REFERENCES

1. Nejman, D., Livyatan, I., Fuks, G., Gavert, N., Zwang, Y., Geller, L.T., Rotter-Maskowitz, A., Weiser, R., Mallel, G., Gigi, E., et al. (2020). The human tumor microbiome is composed of tumor type-specific intracellular bacteria. Science *368*, 973–980. https://doi.org/10.1126/science.aay9189.
2. Galeano Niño, J.L., Wu, H., LaCourse, K.D., Kempchinsky, A.G., Baryiames, A., Barber, B., Futran, N., Houlton, J., Sather, C., Sicinska, E., et al. (2022). Effect of the intratumoral microbiota on spatial and cellular heterogeneity in cancer. Nature *611*, 810–817. https://doi.org/10.1038/s41586-022-05435-0.
3. Castellarin, M., Warren, R.L., Freeman, J.D., Dreolini, L., Krzywinski, M., Strauss, J., Barnes, R., Watson, P., Allen-Vercoe, E., Moore, R.A., and Holt, R.A. (2012). Fusobacterium nucleatum infection is prevalent in human colorectal carcinoma. Genome Res. *22*, 299–306. https://doi.org/10.1101/gr.126516.111.
4. Yamamura, K., Baba, Y., Nakagawa, S., Mima, K., Miyake, K., Nakamura, K., Sawayama, H., Kinoshita, K., Ishimoto, T., Iwatsuki, M., et al. (2016). Human Microbiome Fusobacterium Nucleatum in Esophageal Cancer Tissue Is Associated with Prognosis. Clin. Cancer Res. *22*, 5574–5581. https://doi.org/10.1158/1078-0432.ccr-16-1786.
5. Mitsuhashi, K., Nosho, K., Sukawa, Y., Matsunaga, Y., Ito, M., Kurihara, H., Kanno, S., Igarashi, H., Naito, T., Adachi, Y., et al. (2015). Association of Fusobacterium species in pancreatic cancer tissues with molecular features and prognosis. Oncotarget *6*, 7209–7220. https://doi.org/10.18632/oncotarget.3109.
6. Parhi, L., Alon-Maimon, T., Sol, A., Nejman, D., Shhadeh, A., Fainsod-Levi, T., Yajuk, O., Isaacson, B., Abed, J., Maalouf, N., et al. (2020). Breast cancer colonization by Fusobacterium nucleatum accelerates tumor growth and metastatic progression. Nat. Commun. *11*, 3259. https://doi.org/10.1038/s41467-020-16967-2.
7. Gur, C., Ibrahim, Y., Isaacson, B., Yamin, R., Abed, J., Gamliel, M., Enk, J., Bar-On, Y., Stanietsky-Kaynan, N., Coppenhagen-Glazer, S., et al. (2015). Binding of the Fap2 protein of Fusobacterium nucleatum to human inhibitory receptor TIGIT protects tumors from immune cell attack. Immunity *42*, 344–355. https://doi.org/10.1016/j.immuni.2015.01.010.
8. Brewer, M.L., Dymock, D., Brady, R.L., Singer, B.B., Virji, M., and Hill, D.J. (2019). Fusobacterium spp. target human CEACAM1 via the trimeric autotransporter adhesin CbpF. J. Oral Microbiol. *11*, 1565043. https://doi.org/10.1080/20002297.2018.1565043.
9. Gur, C., Maalouf, N., Shhadeh, A., Berhani, O., Singer, B.B., Bachrach, G., and Mandelboim, O. (2019). Fusobacterium

nucleatum supresses anti-tumor immunity by activating CEACAM1. OncoImmunology *8*, e1581531. https://doi.org/10.1080/2162402x.2019.1581531.

10. Galaski, J., Shhadeh, A., Umaña, A., Yoo, C.C., Arpinati, L., Isaacson, B., Berhani, O., Singer, B.B., Slade, D.J., Bachrach, G., and Mandelboim, O. (2021). Fusobacterium nucleatum CbpF Mediates Inhibition of T Cell Function Through CEACAM1 Activation. Front. Cell. Infect. Microbiol. *11*, 692544. https://doi.org/10.3389/fcimb.2021.692544.
11. Jandus, C., Boligan, K.F., Chijioke, O., Liu, H., Dahlhaus, M., Démoulins, T., Schneider, C., Wehrli, M., Hunger, R.E., Baerlocher, G.M., et al. (2014). Interactions between Siglec-7/9 receptors and ligands influence NK cell-dependent tumor immunosurveillance. J. Clin. Invest. *124*, 1810–1820. https://doi.org/10.1172/jci65899.
12. Carlin, A.F., Lewis, A.L., Varki, A., and Nizet, V. (2007). Group B streptococcal capsular sialic acids interact with siglecs (immunoglobulin-like lectins) on human leukocytes. J. Bacteriol. *189*, 1231–1237. https://doi.org/10.1128/jb.01155-06.
13. Fong, J.J., Tsai, C.M., Saha, S., Nizet, V., Varki, A., and Bui, J.D. (2018). Siglec-7 engagement by GBS β-protein suppresses pyroptotic cell death of natural killer cells. Proc. Natl. Acad. Sci. USA *115*, 10410–10415. https://doi.org/10.1073/pnas.1804108115.
14. Lamprinaki, D., Garcia-Vello, P., Marchetti, R., Hellmich, C., McCord, K.A., Bowles, K.M., Macauley, M.S., Silipo, A., De Castro, C., Crocker, P.R., and Juge, N. (2021). Siglec-7 Mediates Immunomodulation by Colorectal Cancer-Associated Fusobacterium nucleatum ssp. animalis. Front. Immunol. *12*, 744184. https://doi.org/10.3389/fimmu.2021.744184.
15. Chuang, S.S., Kim, M.H., Johnson, L.A., Albertsson, P., Kitson, R.P., Nannmark, U., Goldfarb, R.H., and Mathew, P.A. (2000). 2B4 stimulation of YT cells induces natural killer cell cytolytic function and invasiveness. Immunology *100*, 378–383. https://doi.org/10.1046/j.1365-2567.2000.00031.x.
16. Kaplan, C.W., Lux, R., Haake, S.K., and Shi, W. (2009). The Fusobacterium nucleatum outer membrane protein RadD is an arginine-inhibitable adhesin required for inter-species adherence and the structured architecture of multispecies biofilm. Mol. Microbiol. *71*, 35–47. https://doi.org/10.1111/j.1365-2958.2008.06503.x.
17. Edwards, A.M., Grossman, T.J., and Rudney, J.D. (2007). Association of a high-molecular weight arginine-binding protein of Fusobacterium nucleatum ATCC 10953 with adhesion to secretory immunoglobulin A and coaggregation with Streptococcus cristatus. Oral Microbiol. Immunol. *22*, 217–224. https://doi.org/10.1111/j.1399-302X.2006.00343.x.
18. Wu, C., Chen, Y.W., Scheible, M., Chang, C., Wittchen, M., Lee, J.H., Luong, T.T., Tiner, B.L., Tauch, A., Das, A., and Ton-That, H. (2021). Genetic and molecular determinants of polymicrobial interactions in Fusobacterium nucleatum. Proc. Natl. Acad. Sci. USA *118*, e2006482118. https://doi.org/10.1073/pnas.2006482118.
19. Alphey, M.S., Attrill, H., Crocker, P.R., and van Aalten, D.M.F. (2003). High resolution crystal structures of Siglec-7. Insights into ligand specificity in the Siglec family. J. Biol. Chem. *278*, 3372–3377. https://doi.org/10.1074/jbc.M210602200.
20. Yoshimura, A., Hatanaka, R., Tanaka, H., Kitajima, K., and Sato, C. (2021). The conserved arginine residue in all siglecs is essential for Siglec-7 binding to sialic acid. Biochem. Biophys. Res. Commun. *534*, 1069–1075. https://doi.org/10.1016/j.bbrc.2020.10.023.
21. Yoshimura, A., Asahina, Y., Chang, L.Y., Angata, T., Tanaka, H., Kitajima, K., and Sato, C. (2021). Identification and functional characterization of a Siglec-7 counter-receptor on K562 cells. J. Biol. Chem. *296*, 100477. https://doi.org/10.1016/j.jbc.2021.100477.
22. Lewis, A.L., Robinson, L.S., Agarwal, K., and Lewis, W.G. (2016). Discovery and characterization of *de novo* sialic acid biosynthesis in the phylum Fusobacterium. Glycobiology *26*, 1107–1119. https://doi.org/10.1093/glycob/cww068.
23. Yamakawa, N., Yasuda, Y., Yoshimura, A., Goshima, A., Crocker, P.R., Vergoten, G., Nishiura, Y., Takahashi, T., Hanashima, S., Matsumoto, K., et al. (2020). Discovery of a new sialic acid binding region that regulates Siglec-7. Sci. Rep. *10*, 8647. https://doi.org/10.1038/s41598-020-64887-4.
24. Shao, J.Y., Yin, W.W., Zhang, Q.F., Liu, Q., Peng, M.L., Hu, H.D., Hu, P., Ren, H., and Zhang, D.Z. (2016). Siglec-7 Defines a Highly Functional Natural Killer Cell Subset and Inhibits Cell-Mediated Activities. Scand. J. Immunol. *84*, 182–190. https://doi.org/10.1111/sji.12455.
25. Nordström, T., Movert, E., Olin, A.I., Ali, S.R., Nizet, V., Varki, A., and Areschoug, T. (2011). Human Siglec-5 inhibitory receptor and immunoglobulin A (IgA) have separate binding sites in streptococcal beta protein. J. Biol. Chem. *286*, 33981–33991. https://doi.org/10.1074/jbc.M111.251728.
26. Bullman, S., Pedamallu, C.S., Sicinska, E., Clancy, T.E., Zhang, X., Cai, D., Neuberg, D., Huang, K., Guevara, F., Nelson, T., et al. (2017). Analysis of Fusobacterium persistence and antibiotic response in colorectal cancer. Science *358*, 1443–1448. https://doi.org/10.1126/science.aal5240.
27. Stanietsky, N., Simic, H., Arapovic, J., Toporik, A., Levy, O., Novik, A., Levine, Z., Beiman, M., Dassa, L., Achdout, H., et al. (2009). The interaction of TIGIT with PVR and PVRL2 inhibits human NK cell cytotoxicity. Proc. Natl. Acad. Sci. USA *106*, 17858–17863. https://doi.org/10.1073/pnas.0903474106.
28. Gray-Owen, S.D., and Blumberg, R.S. (2006). CEACAM1: contact-dependent control of immunity. Nat. Rev. Immunol. *6*, 433–446. https://doi.org/10.1038/nri1864.
29. Nicoll, G., Ni, J., Liu, D., Klenerman, P., Munday, J., Dubock, S., Mattei, M.G., and Crocker, P.R. (1999). Identification and characterization of a novel siglec, siglec-7, expressed by human natural killer cells and monocytes. J. Biol. Chem. *274*, 34089–34095. https://doi.org/10.1074/jbc.274.48.34089.
30. Zepeda-Rivera, M., Minot, S.S., Bouzek, H., Wu, H., Blanco-Míguez, A., Manghi, P., Jones, D.S., LaCourse, K.D., Wu, Y., McMahon, E.F., et al. (2024). A distinct Fusobacterium nucleatum clade dominates the colorectal cancer niche. Nature *628*, 424–432. https://doi.org/10.1038/s41586-024-07182-w.
31. Hong, S., Yu, C., Rodrigues, E., Shi, Y., Chen, H., Wang, P., Chapla, D.G., Gao, T., Zhuang, R., Moremen, K.W., et al. (2021). Modulation of Siglec-7 Signaling Via In Situ-Created High-Affinity cis-Ligands. ACS Cent. Sci. *7*, 1338–1346. https://doi.org/10.1021/acscentsci.1c00064.
32. Guo, L., Shokeen, B., He, X., Shi, W., and Lux, R. (2017). Streptococcus mutans SpaP binds to RadD of Fusobacterium nucleatum ssp. polymorphum. Mol. Oral Microbiol. *32*, 355–364. https://doi.org/10.1111/omi.12177.
33. Avril, T., Wagner, E.R., Willison, H.J., and Crocker, P.R. (2006). Sialic acid-binding immunoglobulin-like lectin 7 mediates selective recognition of sialylated glycans expressed on Campylobacter jejuni lipooligosaccharides. Infect. Immun. *74*, 4133–4141. https://doi.org/10.1128/iai.02094-05.
34. Jones, C., Virji, M., and Crocker, P.R. (2003). Recognition of sialylated meningococcal lipopolysaccharide by siglecs expressed on myeloid cells leads to enhanced bacterial uptake. Mol. Microbiol. *49*, 1213–1225. https://doi.org/10.1046/j.1365-2958.2003.03634.x.
35. Engevik, M.A., Danhof, H.A., Auchtung, J., Endres, B.T., Ruan, W., Bassères, E., Engevik, A.C., Wu, Q., Nicholson, M., Luna, R.A., et al. (2021). Fusobacteriumnucleatum Adheres to Clostridioides difficile via the RadD Adhesin to Enhance Biofilm Formation in Intestinal Mucus. Gastroenterology *160*, 1301–1314.e8. https://doi.org/10.1053/j.gastro.2020.11.034.
36. Wu, T., Cen, L., Kaplan, C., Zhou, X., Lux, R., Shi, W., and He, X. (2015). Cellular Components Mediating Coadherence of Candida albicans and Fusobacterium nucleatum. J. Dent. Res. *94*, 1432–1438. https://doi.org/10.1177/0022034515593706.
37. Duev-Cohen, A., Bar-On, Y., Glasner, A., Berhani, O., Ophir, Y., Levi-Schaffer, F., Mandelboim, M., and Mandelboim, O. (2016). The human 2B4 and NTB-A receptors bind the influenza viral hemagglutinin and co-stimulate NK cell cytotoxicity. Oncotarget *7*, 13093–13105. https://doi.org/10.18632/oncotarget.7597.
38. Landolina, N., Zaffran, I., Smiljkovic, D., Serrano-Candelas, E., Schmiedel, D., Friedman, S., Arock, M., Hartmann, K., Pikarsky, E., Mandelboim, O., et al. (2020). Activation of Siglec-7 results in inhibition of *in vitro* and *in vivo* growth of human mast cell leukemia cells. Pharmacol. Res. *158*, 104682. https://doi.org/10.1016/j.phrs.2020.104682.
39. Mandelboim, O., Malik, P., Davis, D.M., Jo, C.H., Boyson, J.E., and Strominger, J.L. (1999). Human CD16 as a lysis receptor mediating direct natural killer cell cytotoxicity. Proc. Natl. Acad. Sci. USA *96*, 5640–5644. https://doi.org/10.1073/pnas.96.10.5640.
40. Javaheri, A., Kruse, T., Moonens, K., Mejías-Luque, R., Debraekeleer, A., Asche, C.I., Tegtmeyer, N., Kalali, B., Bach, N.C., Sieber, S.A., et al. (2016). Helicobacter pylori adhesin HopQ engages in a virulence-enhancing interaction with human CEACAMs. Nat. Microbiol. *2*, 16189. https://doi.org/10.1038/nmicrobiol.2016.189.

STAR★METHODS

KEY RESOURCES TABLE

REAGENT or RESOURCE	SOURCE	IDENTIFIER
Antibodies		
Purified α-human 2B4 (C1.7)	Biolegend	Cat#329502; RRID: AB_1279194
APC α-human CD48 (BJ40)	Biolegend	Cat#336714; RRID: AB_2810517
PE Mouse IgG1, κ Isotype Ctrl Antibody (MOPC-21)	Biolegend	Cat#400112; RRID: AB_2847829
APC Mouse IgG1, κ Isotype Ctrl Antibody (MOPC-21)	Biolegend	Cat#400120; RRID: AB_2888687
PE α-human Siglec-7 (QA79)	Thermo Fisher	Cat#12-5759-42; RRID: AB_11063982
Human serum IgA	Thermo Fisher	Cat#31148; RRID: AB_243597
Alexa Fluor® 647 AffiniPure F(ab') Fragment Donkey Anti-Human IgG	Jackson ImmunoResearch	Cat#709-606-098; RRID: AB_2340580
Allophycocyanin (APC) AffiniPure Goat Anti-Human Serum IgA	Jackson ImmunoResearch	Cat#109-135-011; RRID: AB_2337689
Alexa Fluor® 647 AffiniPure F(ab') Fragment Goat Anti-Mouse IgG (H+L)	Jackson ImmunoResearch	Cat#115-606-146; RRID: AB_2338930
Bacterial and virus strains		
F. nucleatum ATCC 23726	ATCC	N/A
F. nucleatum 23726 ΔRadD	Kaplan et al. (2009), *Mol Microbiol*	N/A
F. nucleatum ATCC 25586	ATCC	N/A
F. nucleatum ATCC 10953	ATCC	N/A
F. nucleatum ATCC 12230	WAL	N/A
F. nucleatum CTI-7	Gur et al. (2015), *Immunity*	N/A
Chemicals, peptides, and recombinant proteins		
TransIT-LT1 Transfection Reagent	Mirus	Cat#MIR 2304
Polybrene Transfection Reagent	Sigma	Cat#TR-1003-G
Neuraminidase *Clostridium perfringens* (*C. welchii*)	Sigma	Cat#N2876-25UN
Octyl-β-D-Glucopyranosid	Sigma	Cat#O8001
Protease Inhibitor Cocktail	Sigma	Cat#P8340
Protein G PLUS-Agarose	Santa Cruz	Cat#sc-2002
Imperial Protein Stain	Thermo Fisher	Cat#24615
Fluorescein-Isothiocyanat Isomer I	Sigma	Cat#7250
Cy®5 Mono 5-pack	Sigma	Cat#PA25001
Arginine	Sigma	Cat#A8094
Lysine	Sigma	Cat#L5501
Calcein AM	Thermo Fisher	Cat#C1413
Experimental models: Cell lines		
721.221	In House	RRID:CVCL_6263
BCBL-1	In House	RRID:CVCL_0165
HEK293T	In House	RRID:CVCL_0063
YTS Eco	In House	RRID:CVCL_EG36
YTS Eco Siglec-7	This study	N/A
Oligonucleotides		
SDM Siglec-7 R124A FWD: ATA CTT CTT TGC TAT GGA GAA AGG AAA TAT AAA ATG GAA TTA TAA ATA TG	Merck	Custom DNA Oligos
SDM Siglec-7 R124A REV: CTC CCC GCA TAC TCA TT	Merck	Custom DNA Oligos

(*Continued on next page*)

Continued

REAGENT or RESOURCE	SOURCE	IDENTIFIER
Recombinant DNA		
pHage-DsRED(-)-eGFP	Addgene	N/A
pHage-DsRED(-)-eGFP Siglec-7	In House	N/A
Software and algorithms		
Prism 6	GraphPad	N/A
FCS Express	*De Novo* Software	N/A

RESOURCE AVAILABILITY

Lead contact

Ofer Mandelboim: oferm@ekmd.huji.ac.il.

Materials availability

Newly generated materials reported in this paper are available from the lead contact upon request.

Data and code availability

Data reported in this paper will be shared by the lead contact upon request. This paper does not report original code. Any additional information required to reanalyze the data reported in this paper is available from the lead contact upon request.

EXPERIMENTAL MODEL AND STUDY PARTICIPANT DETAILS

Cell lines

721.221 cells, BCBL-1 cells, HEK293T cells, and YTS Eco cells were grown in RPMI-1640 medium (Sigma-Aldrich) supplemented with 10% inactivated fetal bovine serum (Sigma-Aldrich), 1 mM sodium pyruvate (Biological Industries), 2 mM glutamine (Biological Industries), nonessential amino acids (Biological Industries), 100 U/ml penicillin (Biological Industries) and 0.1 mg/ml streptomycin (Biological Industries). Cells were cultured in a humidified incubator at 37°C with 5% CO2.

The cells used were regularly authenticated through flow cytometry staining for commonly known markers and tested for mycoplasma contaminations.

Bacteria

The bacterial strains used in this study were *F. nucleatum* subsp. *nucleatum* ATCC 23726 and ATCC 25586, *F. nucleatum* subsp. *polymorphum* ATCC 10953, transtracheal isolate 12230, and tumor isolate *F. nucleatum subsp. nucleatum* CTI-7. The generation of the ΔRadD *F. nucleatum* subsp. *nucleatum* ATCC 23726 gene deletion mutant[16] and the ΔRadD *F. nucleatum* subsp. *polymorphum* ATCC 10953 gene deletion mutant[32] are described elsewhere. Bacteria were kept in −80°C frozen glycerol stocks and grown at 37°C on anaerobic blood agar plates (Novamed) in an anaerobic chamber generated using the Oxoid AnaeroGen anaerobic gas generator system (Thermo Fisher). Bacteria were harvested from blood agar plates for subsequent experimental procedures.

METHOD DETAILS

Generation of YTS cell lines

YTS cell lines were established using lentiviruses generated via the TransIt-LT1 transfection system. To this end, the lentiviral vector pHage-DsRED(–)-eGFP(+) alone (empty vector; EV) or the vector containing the human Siglec-7 gene were used. In brief, HEK293T cells were seeded at 4 – 5 × 10^5 cells/ml in 2 ml complete medium in a 6 well plate 24 hours before transfection. The following day, 0.5 μg of the VSV-G envelope expressing plasmid, 0.5 μg of the gag-pol packaging plasmid psPAX2 and 1 μg of the respective lentiviral vector construct were prepared and combined with 200 μl of Opti-MEM medium. Next, the mixture was incubated with 6 μl of TransIt-LT1 transfection reagent (Mirus) for 10 minutes at room temperature before being added drop-wise to the 6 well plate containing HEK293T cells. Cells were then incubated at 37°C in 5% CO_2.

Four days after transfection, the supernatants containing the lentiviruses were collected and filtered through a 0.42 μm filter. Lentiviruses were used to transduce YTS cells. In brief, 1 ml of the lentivirus preparation was added to 2 ml of fresh RPMI in a 6 well plate. Next, 0.5 ml of YTS cells at 500.000 cells/ml were added to each well. Finally, polybrene was supplemented at 6 μg/ml per well. After expansion of transduced YTS cells, they were sorted according to their GFP expression using a Sony SH800S cell sorter.

De-sialylation of *Fnn* 23726

For the purpose of de-sialylation, bacteria were washed twice with PBS and resuspended in HEPES-buffered saline. Neuraminidase (from Clostridium perfringens; Sigma N2876-25UN) was added for a final concentration of 100 mU/ml (with bacteria at OD1). Bacteria were incubated for 16 hours at 37°C with mild shaking. Next, bacteria were washed an labeled with FITC as described below.

Fusion proteins

To generate fusion proteins, the extracellular portion of the protein of interest was cloned into a mammalian expression vector containing the mutated Fc portion of human IgG1 (CSI-Ig IRES-Puro Fc mut N197A). The generation of human Siglec-7-Ig, human NTB-A-Ig, human 2B4-Ig, human CD16-Ig, human CEACAM1-Ig, and human CEACAM1 ΔN-Ig was described previously.[37–40] Fusion proteins were generated in HEK293T cells and purified using Protein A/G-Sepharose affinity Chromatography. To generate human Siglec-7 R124A-Ig, we used the CSI-Ig (Fc mut N297A)-IRES-Puro Siglec-7 construct as a template. The point mutation was generated by PCR-based site-directed mutagenesis using the forward primer ATA CTT CTT TGC TAT GGA GAA AGG AAA TAT AAA ATG GAA TTA TAA ATA TG and the reverse primer CTC CCC GCA TAC TCA TT.

Immunoprecipitation of *F. nucleatum* RadD using fusion proteins

Fusobacterium nucleatum subsp. *nucleatum* ATCC 23726 WT or its ΔRadD derivative were grown on blood agar plates as described above. Bacteria were washed twice and resuspended at an OD 600 of 6 in 3 ml of lysis buffer (coaggregation buffer (150 mM NaCl, 1 mM Tris-HCl (pH 8), 0.1 mM $CaCl_2$, 0.1 mM $MgCl_2$) supplemented with octyl-glucopyranoside (100mM) and protease inhibitor cocktail (1:200, Sigma Aldrich)). Lysis was performed overnight at 4°C with end-over-end rotation. Following cell lysis, cell debris was removed by centrifugation (5000 g for 8 minutes followed by 21000 g for 12 min). Approximately 500 μg of lysate were mixed with 1 μg of the indicated fusion protein and incubated for 1 hour at 4°C with end-over-end rotation. After 1 hour, protein G-plus beads were added and incubated overnight at 4°C with end-over-end rotation. The following day, immunoprecipitates were collected by centrifugation at 1000 g for 5 minutes at 4°C. Pellets were washed 4 times with coaggregation buffer. The pellets were resuspended in 40 μl of 2x electrophoresis buffer. Elution was performed by boiling samples for 3 minutes. After centrifugation, 20 μl of eluates were separated by 7.5% SDS-PAGE and stained with Imperial protein stain (Thermo Fisher Scientific, Waltham, MA). Immunoprecipitated bands were excised and analyzed by mass spectrometry (at the Smoler Proteomics Center, Department of Biology, Technion Institute of Technology, Haifa).

FITC-labeling of bacteria and flow cytometry

For flow cytometry assays, we labeled bacteria with FITC and gated on the FITC-positive population to discriminate bacteria from debris. Bacteria were harvested from blood agar plates, washed twice and incubated with 0.1 mg/ml FITC (Sigma-Aldrich) in PBS at room temperature in the dark for 30 minutes on a shaker. Subsequently, bacteria were washed three times in PBS at 4000 rpm for 10 minutes to remove unbound FITC. Next, bacteria were divided into 96-well U plates at 1 million bacteria per well and incubated with the indicated amount of fusion proteins (2 μg per well if not stated otherwise) for 1 hour on ice followed by washing and 30 minutes incubation with Alexa Fluor 647-conjugated donkey anti-human IgG or Allophycocyanin (APC) AffiniPure Goat Anti-Human Serum IgA (Jackson Immunoresearch). Histograms of bacteria were gated on FITC-positive cells.

For arginine or lysine blocking experiments, incubation with fusion proteins was performed in the presence of increasing concentrations of arginine or lysine (5 mM, 10 mM, 20 mM, 40 mM). For human serum IgA blocking experiments, bacteria were first incubated with increasing amounts of human serum IgA (0.5 μg, 1 μg, 2 μg, 4 μg) for 1 hour on ice. Next, bacteria were incubated with 0.2 μg of Siglec-7-Ig. Following washing, bacteria were stained with Alexa Fluor 647-conjugated donkey anti-human IgG (does not recognize human serum IgA). Values obtained without blocking antibody were arbitrarily set to 1 and all other values were normalized accordingly.

For antibody blocking experiments, 2μg of fusion proteins were pre-incubated with 1 μg of α-human Siglec-7 (clone S7.7) for 1 hour on ice.

Cy5-labeling of bacteria and cell binding assay

For *F. nucleatum* binding assays, bacteria were labeled with Cy5 (PA25001 Life Sciences GE) solution diluted 0.1 mg/ml in PBS. Analogous to FITC staining, bacteria were labeled with Cy5 for 30 minutes followed by three washes in PBS at 4000 rpm for 10 minutes. We opted for Cy5 staining for adhesion assays since FITC would have interfered with YTS cell GFP fluorescence in flow cytometry. For binding assays, 100.000 YTS cells were incubated with 1 million bacteria in a total of 100 μl per well and incubated for 1 hour on ice. Cells were washed and bacterial binding was detected using a Cytoflex Flow Cytometer and analyzed by FCS express Version 6.

Calcein killing assay

Bacteria were harvested from blood agar plates and washed twice. Target cells were labeled with Calcein-AM for 30 minutes at 37°C in RPMI without supplements. Cells were washed and plated in a 96 U well plate at 5000 cells/well. YTS cells were preincubated with bacteria for 30 minutes at 37°C at a ratio of 1:10 (cells:bacteria). Effector cells with or without bacteria were then incubated with target cells at an E:T ratio of 10:1 for 4 hours at 37°C in RPMI with supplements. Maximal killing was determined by adding NaOH at a final concentration of 100 mM to the target cells (with or without bacteria) and spontaneous release was determined by adding only target cells (with or without bacteria). Following incubation, plates were centrifuged (1000 rpm for 5 min, 4°C) and supernatants (75 μl) were transferred to a black 96 well plate.

The Calcein-AM release into the supernatant was measured using a Tecan Spark multiplate reader with excitation/emission wavelengths at 485nm/535 nm. Specific lysis was calculated as follows: (experimental - spontaneous lysis) / (maximal - spontaneous lysis) x 100.

Cell death staining of YTS cells

YTS cells were incubated with 721.221 or BCBL1 cells (50.000 YTS cells and 5000 target cells) for 4 hours at 37°C in RPMI with supplements. Cells were then washed and stained with Zombie Aqua (Biolegend) at a dilution of 1:500 according to the manufacturer's instructions. Cells were washed and cell death was detected using a Cytoflex Flow Cytometer and analyzed by FCS express Version 6.

QUANTIFICATION AND STATISTICAL ANALYSIS

All statistical analyses were performed using GraphPad Prism 6. A two-tailed unpaired or paired *t* test was used to determine statistical significance of differences between two groups. P-values less than 0.05 were considered statistically significant (* $p \leq 0.05$; ** $p \leq 0.01$; *** $p \leq 0.001$).